research report

Estimation of Restraint Forces for Z-Purlin Roofs Under Gravity Loads

RESEARCH REPORT RP00-4

2000

Committee on Specifications
for the Design of Cold-Formed
Steel Structural Members

American Iron and Steel Institute

The material contained herein has been developed by researchers based on their research findings. The material has also been reviewed by the American Iron and Steel Institute Committee on Specifications for the Design of Cold-Formed Steel Structural Members. The Committee acknowledges and is grateful for the contributions of such researchers.

The material herein is for general information only. The information in it should not be used without first securing competent advice with respect to its suitability for any given application. The publication of the information is not intended as a representation or warranty on the part of the American Iron and Steel Institute, or of any other person named herein, that the information is suitable for any general or particular use or of freedom from infringement of any patent or patents. Anyone making use of the information assumes all liability arising from such use.

ESTIMATION OF RESTRAINT FORCES FOR Z-PURLIN ROOFS UNDER GRAVITY LOADS

By M. C. Neubert[1], Associate Member, ASCE, and T. M. Murray[2], Fellow, ASCE

ABSTRACT: The current specification provisions for the prediction of lateral restraint forces in Z-purlin supported roof systems under gravity loads are in Section D3.1 of the 1996 AISI *Specification for the Design of Cold-Formed Steel Structural Members* (1996). The provisions need refinement, because they are empirical, have an incorrect treatment of roof slope and system effects, and ignore the effect of panel stiffness on restraint forces. Therefore, a new restraint force design procedure, having a stronger reliance on engineering principles, is proposed. Elastic stiffness models, with varying roof slope, panel stiffness, and cross-sectional properties, were used to develop the procedure. A new treatment of Z-purlin statics has led to a more accurate method of addressing roof slope. A system effect factor accounts for the observed nonlinear increase in restraint force with the number of restrained purlins. An adjustment factor varies the predicted restraint force depending on the shear stiffness of the roof panel. The proposed procedure applies to five bracing configurations: support, third-point, midspan, quarter point, and third-point plus support restraints.

Key words: cold-formed steel, metal roof, restraint, Z-purlin

INTRODUCTION

---

[1] Graduate Research Assistant, Dept. of Civil and Envir. Engineering, Virginia Polytechnic Institute and State Univ.
[2] Montague-Betts Professor, Dept. of Civil and Envir. Engineering, Virginia Polytechnic Institute and State Univ.

Section D3.1 of the AISI *Specification for the Design of Cold-Formed Steel Structural Members* (1996) has provisions that predict required brace forces in Z-purlin supported roof systems. The provisions were developed using elastic stiffness models of horizontal (flat) roofs (Elhouar and Murray, 1985) and verified by full-scale and model testing (Seshappa and Murray, 1985). For example, the predicted restraint force in each brace for single span systems with anti-roll restraints only at the supports, Figure 1, is:

$$P_L = 0.5(\beta W) \tag{1}$$

where W = the total applied vertical load (parallel to the web), and

$\beta = \dfrac{0.220 b^{1.5}}{n_p^{0.72} d^{0.90} t^{0.60}}$, and b is purlin flange width, d is depth of section, t is thickness, and

n_p is the number of restrained purlin lines. The restraint force ratio, β, was developed from regression analysis of stiffness model results of Z-purlin supported roof systems.
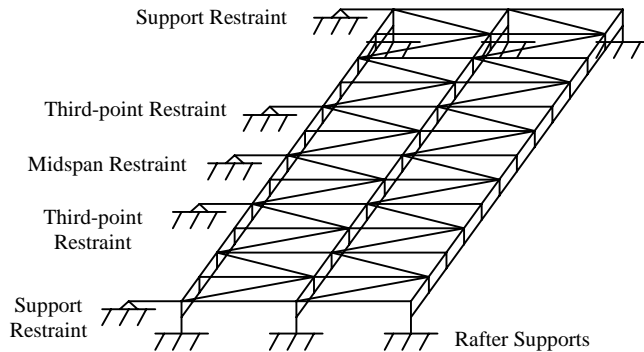

Figure 1. Elastic Stiffness Model

To account for roof slope, the latest balloted AISI provision for the single span, anti-roll restraints only at the supports is:

$$P_L = 0.5(\beta \cos\theta - \sin\theta)W \tag{2}$$

where θ is roof slope measured from the horizontal. The terms $W\cos\theta$ and

$W\sin\theta$ represent the gravity load components parallel and perpendicular to the purlin web as shown in Figure 2, respectively. The latter component is also referred to as the downslope component.
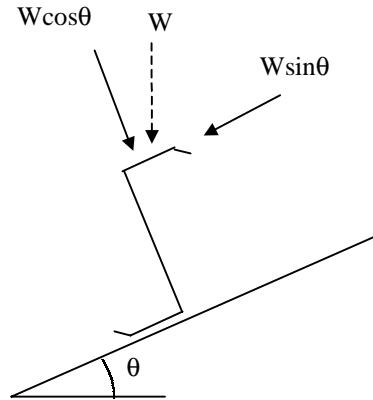

Figure 2. Gravity Load Components

From basic principles (Zetlin and Winter, 1955), the required restraint force is:

$$P_L = 0.5\left(\frac{I_{xy}}{I_x}\right)W \tag{3}$$

where I_{xy} is the product moment of inertia and I_x is the moment of inertia with respect to the centroidal axis perpendicular to the web of the Z-section. The Elhouar and Murray (1985) study showed that the restraint force given by Equation 3 is conservative, that is $I_{xy}/I_x > \beta$, because of system effects. Equation 1 can be rewritten as:

$$P_L = 0.5\alpha\left(\frac{I_{xy}}{I_x}\right)W \tag{4}$$

where $\alpha = \dfrac{I_x}{I_{xy}}\beta$ = system effect factor. Thus, the system effect is identified as a function of the AISI Specification parameter β.

The system effect is the inherent restraint in the system because of purlin web flexural

stiffness and a Vierendeel truss effect caused by interaction of the purlin web with the

roof panel and the rafter flange (see Figure 3). This Vierendeel truss action explains the

relative decrease in restraint force as the number of purlin lines, n_p, increases as shown in

Figure 4. Figure 5 is a plot of restraint force from Equation 2 versus the slope angle θ.

The value θ_0 is the intercept where the restraint force is equal to zero. For roof slopes

less than θ_0, the AISI Specification provision, Equation 2, predicts a restraint force in

tension. For slopes greater than θ_0, Equation 2 predicts the restraint force to be in
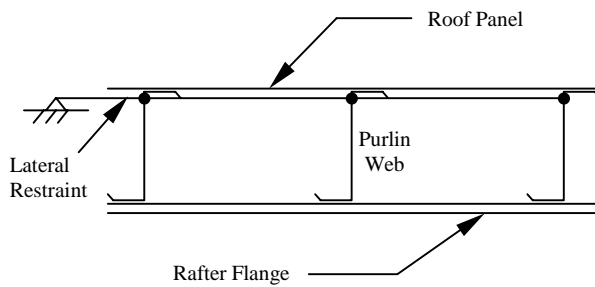
compression.

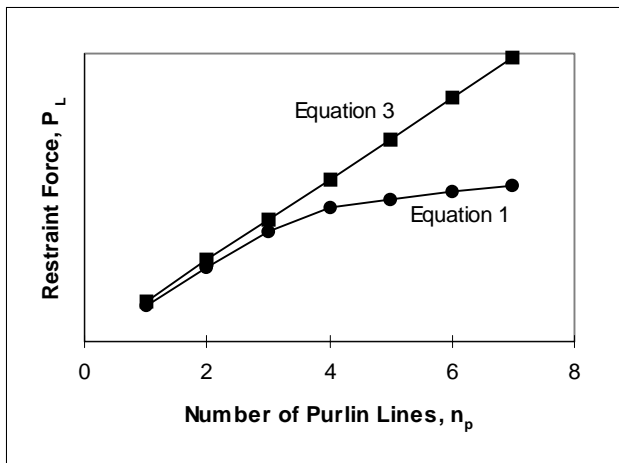**Figure 3. Vierendeel Truss Action**

**Figure 4. Restraint Force vs. Number of Purlin
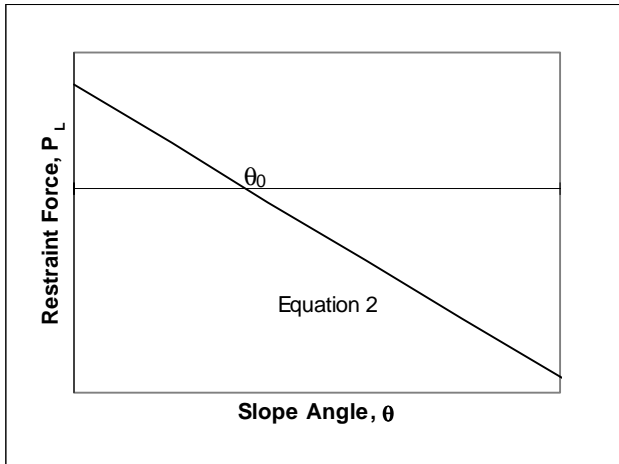Lines – Eqns. 1,3**

Figure 5. Restraint Force vs. Roof Slope – Eqn. 2

Equation 2 has a flawed treatment of both the system effect and roof slope, because two important effects are not taken into account. First, the internal system effect applies to both the fictitious force $W\cos\theta(I_{xy}/I_x)$ and the real force $W\sin\theta$. Second, the system effect reverses when the net restraint force, changes from tension to compression with increasing slope angle. As a result of these effects, the intercept value θ_0 is in actuality dependent only on purlin cross-sectional properties, not n_p or the bracing configuration. However, Equation 2 has θ_0 dependent on β, which is a function of both n_p and the bracing configuration:

$$\theta_0 = \tan^{-1}\beta \tag{5}$$

The elastic stiffness models used to develop the AISI Provisions had an assumed roof panel stiffness of 440 N/mm (2500 lb/in.). For this discussion, roof panel stiffness is defined as:

5

$$G' = \frac{PL}{4a\Delta}$$ (6)

where P is a point load (lb) applied at midspan of a rectangular roof panel, L is the panel's span length, a is the width of the panel, and Δ is the deflection of the panel at the location of the point load. Refer to Figure 6 for a picture of the test setup to calculate panel stiffness. Computer tests run by Elhouar and Murray indicated that the increase in required bracing force for systems with roof panels stiffer than 440 N/mm (2500 lb/in.) was negligible. However, these tests only considered systems with three or fewer restrained purlin lines. After examining stiffness models of roof systems with up to eight restrained purlins, results showed that increasing panel stiffness above 440 N/mm (2500 lb/in.) caused significant increases in the required brace forces for systems with four or more purlin lines. Thus, the AISI Specification should be modified to address roof panels with any common shear stiffness value.
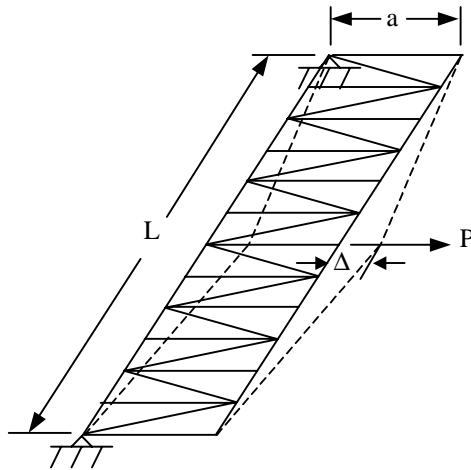


Figure 6. Panel Stiffness Test Setup

MATHEMATICAL MODELING

A large amount of test data, representing the full range of parameters used in Z-purlin

supported roofs, is required to develop and verify design equations for the estimation of restraint force in Z-purlin roof systems. A numerical model is necessary for this research, because the number of experimental tests needed to collect this data would be impractical, and the existing data from previous tests is insufficient. In their research, Elhouar and Murray (1985) used a space frame stiffness model to generate restraint force data for their design equations. Their model, hereafter referred to as the Elhouar and Murray model, is appropriate because solid effects and second order effects have a negligible effect on Z-purlin restraint forces. The model retained the key aspects of the physical system, allowed roof parameters to be easily modified, had a manageable execution time, and showed excellent agreement with experimental results. Therefore, an elastic stiffness model (shown in Figure 1), based on the Elhouar and Murray model, was chosen for this investigation and is hereafter called the current model. Analysis specifications were set such that shear deformations, torsional warping effects, and second order effects were neglected, because this study examines only axial forces. The material used for all elements of the model was linear elastic steel.

Modeling of Purlins

Similar to the Elhouar and Murray model, the current model represents a Z-purlin as a space truss. The truss consists of four different elements, and is divided into twelve sections of equal length (see Figure 7) to provide joints for support, third-point, quarter-point, and midspan lateral restraints.
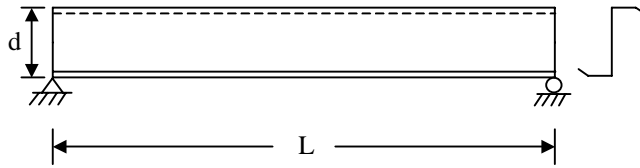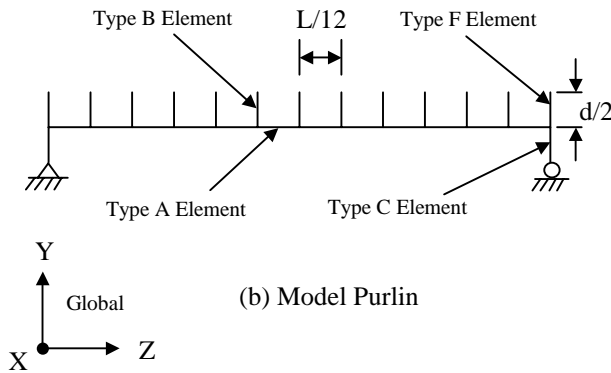
Figure 7. Purlin Modeling

The main purlin elements, oriented along the length of the purlin in the global Z direction, are type A elements. These elements are given different cross-sectional properties depending on the dimensions of the purlin being modeled. The section properties given in Table I-3 of the *Cold-Formed Steel Design Manual* (1996), for standard Z-sections with lips were used, with some adjustments. The torsion constant *J* was set equal to 4.16×10^6 mm^4 (10 in^4) for all cases, to prevent the type A elements from rotating with respect to their adjoining elements and causing extreme and uncharacteristic deformations in the system.

Perpendicular to the type A elements are the type B and F elements, located at the ends of all twelve sections. These elements, having a length of half the purlin depth,

model purlin web bending and connect the main purlin elements (type A) to the roof panel elements (type D). Thus, the model properties are consistent with that of a *L*/12 section of purlin for type B elements, and a *L*/24 section of purlin for type F elements on the outside of each purlin line.

The last purlin element is type C, which connects the purlin to the rafter supports. The model section properties for this member correspond to a *L*/2 length of purlin, except for the z-axis moment of inertia, which was arbitrarily set equal to 4.16×10^5 mm^4 (1 in^4) for all cases. This virtually eliminates bending in the Type C elements, ensuring that all purlin bending takes place in the Type B elements. The rafter supports are located at either end of every purlin span, at the base of all type C elements. In the model, the Z-axis rotation at these boundaries is fixed because the rafter support is assumed to prevent purlin web bending about this axis. In reality, this boundary is a rotational spring, offering significant resistance to purlin web bending, but allowing for some rotation. The effect of using fixed rotation restraint versus rotational springs is beyond the scope of this project, and it is believed to be negligible.

Modeling of Roof Panel

In the current model, roof panel bending stiffness is neglected and only shear stiffness is considered. The roof panel is modeled as a space truss, consisting of 1.52 m (5 ft) wide sections between each purlin line, each with a series of diagonal members (see Figure 8). All of the elements in the roof panel have the same model section properties and are denoted as type D elements. To simulate the lack of bending stiffness, all moments of inertia for type D elements are set equal to zero. The shear stiffness of the roof panel was varied from 175 N/mm (1000 lb/in.) to 17,500 N/mm (100,000 lb/in.). The area of the

type D elements determines the shear stiffness of the roof panel, and thus the area of these elements was varied to get the desired range of shear stiffness values.
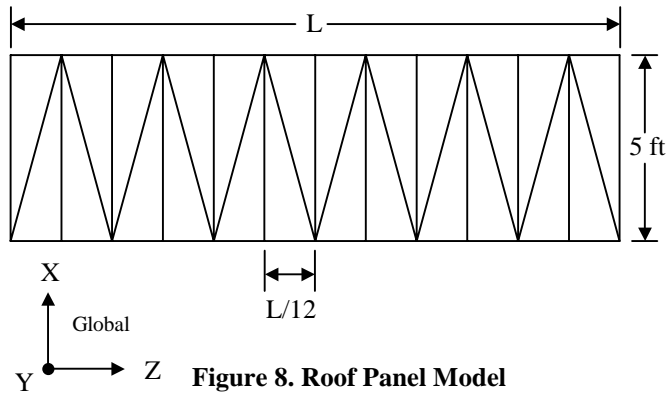
Figure 8. Roof Panel Model (Danza and Murray, 1998)

Modeling of Braces

In the current model, lateral braces for the roof system are axial load only members, and are represented by line elements. To eliminate any bending in these members, referred to as type E elements, the eave connections are given fully pinned boundary conditions, and the restraint to purlin joints are given bending pin releases. For all cases, the area of these elements was arbitrarily set at 215 mm^2 (0.333 in^2), and the element length was set at 203 mm (8 in). These values are intended to represent the typical lateral restraint used in practice and to match the values used in previous studies. Since no bending resistance is required, all moments of inertia for type D elements are set equal to zero.

Modeling of Loads

This discussion deals exclusively with gravity loads and does not address uplift forces. Gravity loads are represented in the current model by sets of distributed line loads

and point moments acting along each purlin line. The total gravity load acting on the roof system, W (N), is distributed equally to all restrained purlin lines such that the load carried by each is $w = 14.6$ N/m (100 plf), for all cases. The distributed load is first split into components parallel and perpendicular to the purlin web, which change depending on the slope angle of the roof. The distributed load acting parallel to the web, w_{web}, was then split into components (w_y and w_z) along each of the principle axes (defined by the angle θ_p) of the type A elements (see Figure 9). The distributed load acting perpendicular to the web, also known as the downslope component, w_{ds}, is applied to the type D panel elements on top of each purlin line.
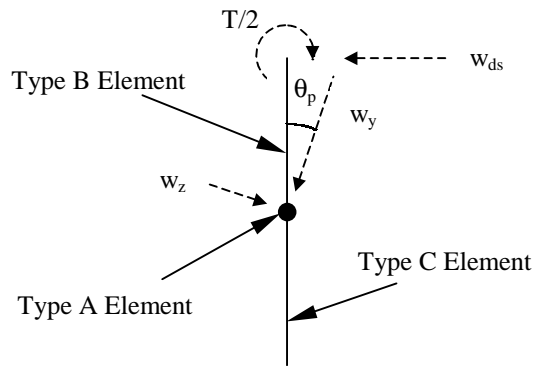
Figure 9. Model Purlin Loads

Due to roof slope and the asymmetry of the Z-purlin cross-section, purlins connected to sheathing receive an eccentric loading. The magnitude of this eccentricity, measured along the purlin top flange, determines the torque loading on each purlin line. The true load distribution on the purlin top flange is unknown, but for this model, an eccentricity of one third of the purlin flange width was assumed, as used by Elhouar and Murray (1985). A comparison of theoretical and experimental results by Ghazanfari and Murray (1983) confirmed the validity of this assumption. From statics, the total torque acting on

11

each purlin span is:

$$T = \frac{bw_{web}L}{3}$$ (7)

where T is the total torque (N-m), b is the flange width (m), and L is the span length (m).

A series of point moments is applied to the joints of the type D roof panel elements.

Applying moments at the purlin to roof panel connection allows these moments to be properly transferred to the restraints. The total torque is then distributed equally to every joint along each purlin span.

THEORETICAL DEVELOPMENT OF DESIGN EQUATION

To develop a more accurate set of equations to predict the lateral restraint force in Z-purlin roof systems, the following form was assumed:

$$P_L = P_0 C_1 \left(n_p^* \alpha + n_p \gamma \right)$$ (8)

where P_0 is the restraint force on a single purlin system, C_1 is the brace location factor, α is the system effect factor, and γ is the panel stiffness factor. The parameter n_p^* is closely related to n_p, as will be described later. Equation 8 postulates that the predicted restraint force in any given system is equal to the force on a single purlin multiplied by the total number of purlins, a brace location factor, a reduction factor caused by system effects, and modified by a factor for roof panel stiffness. This equation was formulated by first considering a roof panel stiffness of 440 N/mm (2500 lb/in.) to obtain a base point along the brace force versus panel stiffness curve (see Figure 10). Notice that Figure 10 is shown with panel stiffness in a log scale. When $G' = 440$ N/mm (2500 lb/in.), $\gamma = 0$ and Equation 8 reduces to:
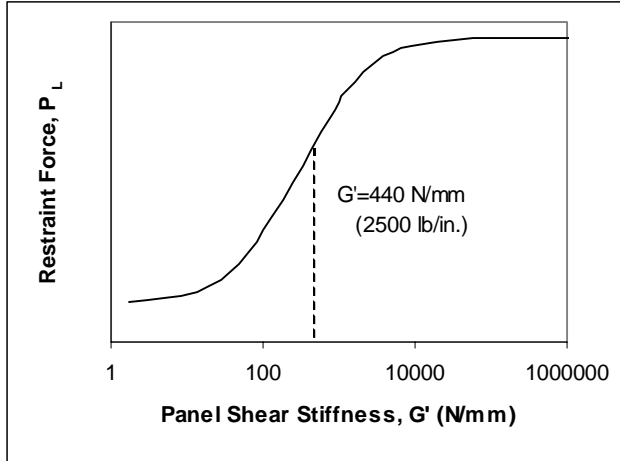
$$P_L = P_0 C_1 n_p^* \alpha$$ (9)

Figure 10. Restraint Force vs. Panel Stiffness (Model)

To predict the base point restraint force, the diagram in Figure 11 is now used to develop an expression for P_0 that considers the proper application of the system effect and its reversal. The key assumption to this model is that the purlin has a pinned support at the rafter connection. W_p is the total gravity load acting on each purlin span:

$$W_p = wL \tag{10}$$

where w is the distributed gravity load on each purlin (force/length) and L is the span length. The fictitious force $W_p(I_{xy}/I_x)$ is the overturning force from basic principles (Zetlin and Winter, 1955). Figure 11 shows the set of real and fictitious forces associated with a single purlin on a roof with slope θ. The set of forces accounts for the following effects: $W_p\sin\theta$ is the downslope component of the gravity loading, $W_p\cos\theta(I_{xy}/I_x)$ is the fictitious force as previously discussed, and $W_p\cos\theta(b/3)$ is the torque induced by eccentric loading of the top flange. Summation of moments about the pinned support

13

results in:

$$P_0 = \left[\left(\frac{I_{xy}}{2I_x} + \frac{b}{3d}\right)\cos\theta - \sin\theta\right]W_p \tag{11}$$

which is valid if P_0 is positive (tension) or negative (compression). Solving for the intercept slope angle, where restraint force is zero:

$$\theta_0 = \tan^{-1}\left(\frac{I_{xy}}{2I_x} + \frac{b}{3d}\right) \tag{12}$$

Thus, the intercept is dependent only on purlin cross-sectional properties as required. For roof slopes less than θ_0, P_0 is in tension, and for roof slopes greater than θ_0, P_0 is in compression.

$W_p\cos\theta$

$W_p\sin\theta$

P_L

$W_p\cos\theta(b/3)$

$W_p\cos\theta(I_{xy}/I_x)$
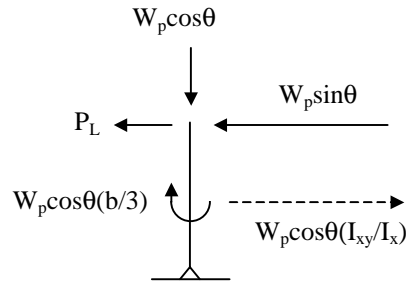
Figure 11. Purlin Gravity Loads

When Elhouar and Murray (1985) used regression analysis to derive Equation 4, they assumed that the system effect factor, α, was dependent on the following parameters: $I_{xy,}$ $I_{x,}$ b, n_p, d, and t. However, if the system effect is taken to be caused purely by purlin bending resistance, then only the parameters n_p, d, and t should affect α. Statistical analysis, based on stiffness model results, was used to develop a new equation for α:

$$\alpha = 1 - C_2\left(\frac{t}{d}\right)\left(n_p^* - 1\right) \tag{13}$$

where C_2 is a constant factor. Note that α is a dimensionless factor and $\alpha=1$ when $n_p^*=1$, as needed for consistency. Since α is a multiplicative factor in Equation 8, it accurately models the reversal of the system effect when P_0 changes from tension to compression.

For a rational basis to Equation 13, consider a purlin to be a cantilevered, rectangular beam with a point load acting at the free end (see Figure 12). The deflection of such a beam is proportional to the ratio $(d/t)^3$, and since α is a measure of bending resistance it is proportional to $(t/d)^3$. This, though, does not consider the effects of panel restraint, and elastic stiffness model results indicate that the slope of α has an approximately linear variation with t/d. The coefficient C_2 in front of t/d in Equation 13 was determined from a regression analysis, and its values are tabulated in Appendix III. This coefficient differs for each bracing configuration because bending resistance changes depending on a brace's distance from rafter supports and other braces.
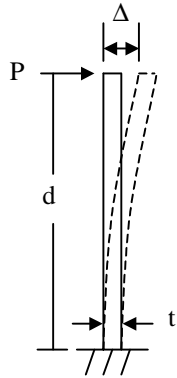

Figure 12. Purlin Web Bending

Observe that Equation 9 is quadratic with respect to n_p, because α is linear in n_p. Thus, for some value of n_p, denoted as $n_{p(max)}$, P_L will reach a maximum point and then decrease as n_p is increased above $n_{p(max)}$. From basic calculus, $n_{p(max)}$ can be determined:

$$n_{p(max)} = 0.5 + \frac{d}{2C_2 t} \tag{14}$$

Obviously, the required bracing force can never decrease as the number of purlins is increased. This concern can be eliminated by using n_p^* instead of n_p in Equation 9, where n_p^* is defined as the minimum of $n_{p(max)}$ and n_p. This means that adding additional purlin lines above $n_{p(max)}$ will not affect the predicted restraint force; P_L will remain constant (see Figure 13).
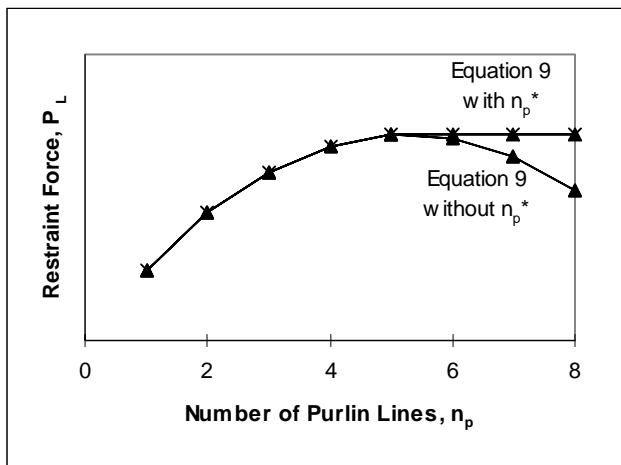
Figure 13. Effect of Using n_p^*

Another key element in Equation 9 is C_1, the brace location factor. This constant factor represents the percentage of total restraint that is allocated to each brace in the system. Therefore, the sum of the C_1 coefficients for each brace in one purlin span length is approximately equal to unity. The values for C_1 were determined from a regression analysis and are tabulated for various bracing schemes in the Appendix III. Notice that for multiple span systems, the C_1 values are larger for exterior restraints than the corresponding interior restraints, as expected from elementary mechanics.

Equation 9 establishes the restraint force for the base point of $G' = 440$ N/mm (2500

lb/in.).   Figure 14 shows a plot comparing the proposed Equation 9 to the AISI

Specification, Equation 2 with respect to slope angle θ.   Figure 15 shows a similar plot

with respect to the number of restrained purlin lines.

Figure 14. Restraint Force vs. Roof Slope – Eqns. 2, 9

**Figure 15. Restraint Force vs. Number of
Purlins – Eqns. 2, 9**

To extend Equation 9 to the general form in Equation 8, a panel stiffness modifier, γ,

is included. After analyzing several different cases, lateral restraint force was shown to
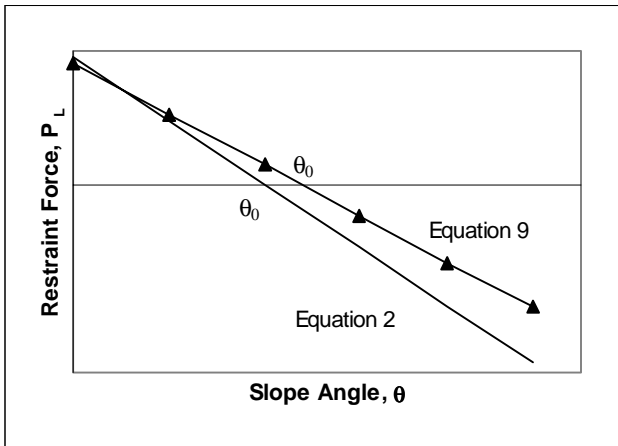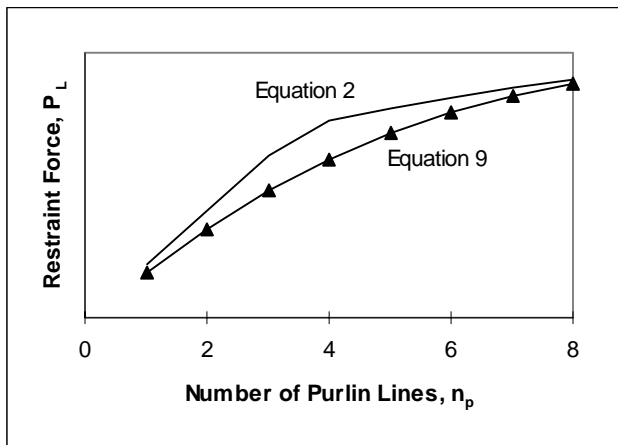
vary linearly with the common logarithm of the roof panel stiffness over the range of common panel shear stiffnesses (refer to Figure 10). This lead to the following equation for the panel stiffness modifier:

$$\gamma = C_3 \log\left(\frac{G'}{440 \text{ N/mm}}\right) \tag{15}$$

where G' is the roof panel shear stiffness (N/mm) and C_3 is a constant determined by regression analysis of stiffness model results. In Equation 15, the denominator constant of 440 has units of N/mm to nondimensionalize the term in the log parentheses when G' is in units of N/mm. When G' is in lb/in., the converted denominator constant is 2500. For roof panels stiffer than the base point value, the required restraint force is increased, and for panels less stiff than the base value, the required restraint force is decreased. The values of C_3 are tabulated for various bracing schemes in Appendix III. The location of a brace with respect to rafter supports and other braces determines how the restraint force varies with roof panel stiffness. Notice in Equation 8 that γ is multiplied by n_p instead of n_p^*, because as panel stiffness changes, change in restraint force depends on the total number of purlins in the system and $n_{p(max)}$ no longer applies.

To utilize the panel stiffness modifier, two restrictions are required. First, γ is valid only for 175 N/mm (1000 lb/in.) $\leq G' \leq$ 17,500 N/mm (100,000 lb/in.). This is the range of linear behavior, and most roof panels have shear stiffnesses within this limitation. Second, a maximum restraint force is set, which can never be exceeded. This maximum force is:

$$\left|P_L\right| \leq \left|P_0 C_1 n_p\right| \tag{16}$$

and is the expected restraint force if system effects are ignored. See Figure 16 for a

typical plot of restraint force versus panel stiffness for Equation 8, shown with stiffness model results.
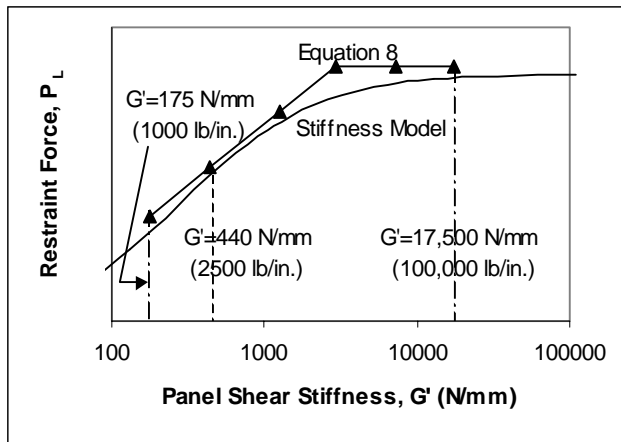
Figure 16. Restraint Force vs. Panel Stiffness –
Eqn. 8 and Model

Restrictions must also be placed on Equation 8 to make it applicable for design purposes. Since the stiffness models used to confirm the equation had eight restrained purlin lines or fewer, Equation 8 must be used with caution when $n_p > 8$. The proposed equation is believed to apply to the design of lateral restraints in roof systems with $n_p > 8$, but further computer testing is require to prove this. When Equation 8 gives a very small predicted magnitude of restraint force, $\left|P_L\right| \leq 445\,\text{N}\,(100\,\text{lb})$, no lateral bracing is necessary. For every Z-purlin supported roof system, there is a range of roof slopes that corresponds to $\left|P_L\right| \leq 445\,\text{N}$, and roofs systems having a roof slope within this range require no lateral restraint.

COMPUTER TESTS AND EQUATION DEVELOPMENT

The theoretical equation developed earlier was then matched to the stiffness model results by evaluating the coefficients C_1, C_2, and C_3. An investigation into roof system behavior was made, determining the effect of each parameter upon the required lateral restraint forces. Then, a computer test matrix was developed to define the range of investigation for each parameter within the current elastic stiffness model. A statistical regression analysis was used to determine the coefficients C_1, C_2, and C_3 of the proposed design equation for each bracing configuration.

In the computer test matrix, five different lateral bracing configurations were examined: support, third-point, midpoint, quarter-point, and third-point plus support restraints. Different equation coefficients are necessary for single and multiple span conditions, so a one span and a three span model were created for each bracing configuration. A total of ten different purlins were selected for the computer test matrix. The dimensions of these purlins are given in Table 1 – there are six different cross-sections and five different span lengths. These purlin dimensions were chosen as being representative of the typical range of purlins used in industry. Span length is varied independently of purlin cross-section. Two different purlin thicknesses were chosen for the 203 mm (8 in.) and 254 mm (10 in.) deep purlins, to examine the effects of varying the thickness to depth ratio. The purlins P1 and P10 were selected to represent extreme cases; P1 is a very thin and deep purlin ($t/d = 0.005$) while P10 is a very thick and shallow purlin ($t/d = 0.0175$). These extreme cases are included to ensure that the design equations accurately predict restraint forces for any typical purlin section and span length. Complete section properties for each of the purlin cross-sections are found in the *Cold*

Formed Steel Design Manual (1996).

Table 1. Purlin Dimensions

ID	Section	d mm (in.)	b mm (in.)	t mm (in.)	L m (ft)
P1	12ZS3.25x060	305 (12)	82.6 (3.25)	1.52 (0.060)	10.97 (36)
P2	10ZS3x135	254 (10)	76.2 (3.00)	3.43 (0.135)	10.67 (35)
P3	10ZS3x135	254 (10)	76.2 (3.00)	3.43 (0.135)	9.14 (30)
P4	10ZS3x075	254 (10)	76.2 (3.00)	1.91 (0.075)	10.67 (35)
P5	10ZS3x075	254 (10)	76.2 (3.00)	1.91 (0.075)	9.14 (30)
P6	8ZS2.5x090	203 (8)	63.5 (2.50)	2.29 (0.090)	7.62 (25)
P7	8ZS2.5x090	203 (8)	63.5 (2.50)	2.29 (0.090)	6.10 (20)
P8	8ZS2.5x060	203 (8)	63.5 (2.50)	1.52 (0.060)	7.62 (25)
P9	8ZS2.5x060	203 (8)	63.5 (2.50)	1.52 (0.060)	6.10 (20)
P10	6ZS2x105	152 (6)	50.8 (2.00)	2.67 (0.105)	6.10 (20)

The next parameter in the test matrix is the number of parallel restrained purlin lines. For flat roofs (zero slope), the number of restrained purlin lines tested was one to eight, inclusive. Note that in practice, the number of purlin lines between restraint anchors rarely exceeds eight. For models with eight restrained purlin lines, the computer tests varied both the roof slope and the roof panel shear stiffness, independently of each other. Eleven different roof slopes were tested; 0:12, ½:12, 1:12, 2:12, … 9:12. For models with n_p=8 and θ=0, six different roof panel shear stiffnesses were tested. The values of roof panel stiffness used for each span length are shown in Table 2, and these values are typical for actual roof panels and cover the range of log-linear behavior. All span lengths include the shear stiffness of 440 N/mm (2500 lb/in.), the base point used to formulate the design equations. The set of computer test combinations for roof slope, panel shear stiffness, and number of restrained purlin lines is summarized in Table 3 below. The designations G1 through G6 refer to the panel shear stiffness values given in Table 2.

The models for this set of combinations were analyzed for each bracing configuration, number of spans, and purlin in the test matrix.

Table 2. Panel Shear Stiffness Values

ID	L=20 ft	L=25 ft	L=30 ft	L=35 ft	L=36 ft
G1	13469 (76923)	12875 (73529)	11419 (65217)	9885 (56452)	9849 (56250)
G2	4072 (23256)	3908 (22321)	3502 (20000)	3004 (17157)	2918 (16667)
G3	1357 (7752)	1303 (7440)	1162 (6637)	1001 (5719)	970 (5538)
G4	818 (4673)	779 (4448)	813 (4644)	701 (4005)	679 (3879)
G5	438 (2500)	437 (2495)	438 (2500)	438 (2500)	438 (2500)
G6	273 (1560)	260 (1486)	232 (1326)	200 (1145)	194 (1109)

Note: Panel Stiffnesses in N/mm (lb/in.)

Table 3. Combinations of n_p, θ, and G'

Combination	n_p	Roof Slope	G'
1	8	0:12	G5
2	8	½:12	G5
3	8	1:12	G5
4	8	2:12	G5
5	8	3:12	G5
6	8	4:12	G5
7	8	5:12	G5
8	8	6:12	G5
9	8	7:12	G5
10	8	8:12	G5
11	8	9:12	G5
12	1	0:12	G5
13	2	0:12	G5
14	3	0:12	G5
15	4	0:12	G5
16	5	0:12	G5
17	6	0:12	G5
18	7	0:12	G5
19	8	0:12	G1
20	8	0:12	G2
21	8	0:12	G3
22	8	0:12	G4
23	8	0:12	G6

The current stiffness model used to represent Z-purlin supported roof systems is linear and elastic, so the restraint force is linearly proportional to the applied load. Arbitrarily, a uniform gravity load of w=1459 N/m (100 plf) was applied to every purlin line for all models in the test matrix.

In summary, the test matrix consists of 2300 computer model tests. This total comes from five bracing configurations (BC), two numbers of continuous spans (S), ten purlins(P), 23 parameter combinations (PC), and one loading (L):

$$[5BC]x[2S]x[10P]x[23PC]x[1L] = 2300 \text{ tests} \tag{17}$$

Statistical Analyses

Engineering principles were used to derive the form of the proposed restraint force design equation. The only components of the equation that remain to be defined are the coefficients C_1, C_2, and C_3. These coefficients are different for each brace location in each lateral restraint configuration. The results of the computer test matrix provide enough data to accurately determine the values of these coefficients, but a means of statistical analysis is necessary to process this data. The form of the proposed design equation requires that a multivariable, nonlinear regression analysis be performed.

A weighted, least-squares regression was chosen to analyze the data. Because the computer test matrix includes different roof slopes, some restraint force results are positive (tension) while others are negative (compression). Also, the magnitude of some restraint force results is many times greater than others. To create design equations with the smallest percent error, a weighted regression (based on the absolute value of the restraint force given by the stiffness model) was used to determine the unknown coefficients.

Two separate regression analyses were performed; a constant panel stiffness regression and a variable panel stiffness regression. The constant panel stiffness regression included all the data points where G'=2500 lb/in. (combinations 1 through 18 in Table 3). The variable panel stiffness regression included all the data points where G' is varied (combinations 1 and 19 through 23 in Table 3). The design equation summarized in Appendix III was the regression equation used for both analyses.

As a means of evaluating the effectiveness of the regression model in describing the computer test data, the statistical term R^2 was used. R^2 is the coefficient of determination, which varies from zero (no relationship exists between the regression model and the test data) to one (the regression model perfectly predicts the test data). For this research, values of R^2 greater than 0.90 were deemed acceptable for determining the regression coefficients.

To determine final coefficient values for the proposed design equation, three regression trials were performed. For the first trial, only the constant panel stiffness regression was executed, resulting in initial values of C_1 and C_2 which were then adjusted for design purposes. These adjusted C_2 values were included as known values in the second regression trial, which then calculated revised C_1 values. For this second trial, the constant panel stiffness regression was again performed. The resulting C_1 values from the second trial were adjusted to the nearest appropriate value for design purposes, using two significant digits. For the third trial, the variable panel stiffness regression was performed. The adjusted values for C_1 and C_2 were taken as known quantities, and initial values for the coefficient C_3 were determined. The R^2 values for all three trials were greater than 0.90 for all restraint configurations (see Table 4), except for three cases that

were all above 0.89 and deemed acceptable. After the third regression trial, the final

values of the regression coefficients were determined by adjusting the C_3 values. Again,

these values need only have two significant digits of accuracy, and were adjusted to

appropriate values for use in the design equation. The final regression coefficient values

are presented in Table 5 in Appendix III.

Table 4. R^2 Values for Regression Analyses

Configuration	R^2: 1st Trial	R^2: 2nd Trial	R^2: 3rd Trial
Support Restraints:			
SS	0.9978	0.9978	0.9812
MS, exterior	0.9979	0.9979	0.9803
MS, interior	0.9704	0.9704	0.9830
Third-point Restraints:			
SS	0.9980	0.9978	0.9886
MS, exterior	0.9977	0.9977	0.9830
MS, interior	0.9961	0.9961	0.9701
Midspan Restraints:			
SS	0.9962	0.9961	0.9706
MS, exterior	0.9952	0.9952	0.9430
MS, interior	0.9719	0.9710	0.8986
Quarter-point Restraints:			
SS, exterior	0.9913	0.9913	0.9416
SS, interior	0.9934	0.9931	0.8946
MS, exterior ¼ span	0.9906	0.9906	0.9194
MS, interior ¼ span	0.9883	0.9883	0.8927
MS, ½ span	0.9972	0.9971	0.9571
Third-point Plus Support Restraints:			
SS, exterior	0.9781	0.9781	0.9096
SS, interior	0.9973	0.9973	0.9706
MS, exterior support	0.9838	0.9838	0.9338
MS, interior support	0.9704	0.9704	0.9492
MS, third-point	0.9957	0.9957	0.9426

CONCLUSIONS AND RECOMMENDATIONS

A design procedure has been formulated to predict the required restraint force for Z-

purlin supported roof systems under gravity loads. The procedure accounts for roof

systems of any slope and panel shear stiffness (within a specified range). The procedure applies to single and multiple span systems with the following bracing configurations: support, third-point, midspan, quarter-point, and third-point plus support restraints. The American Iron and Steel Institute's *Specification for the Design of Cold-Formed Steel Structural Members* (1996) has provisions for the prediction of Z-purlin restraint forces. The empirical equations in these provisions lack a strong connection to engineering principles, and have different forms for the final solution. The proposed design procedure is unified for all bracing configurations and is a more accurate representation of Z-purlin roof systems. It is recommended that the current AISI Provisions be revised to include the proposed design procedure.

ACKNOWLEDGEMENTS

APPENDIX I. REFERENCES

Cold-Formed Steel Design Manual, (1996). American Iron and Steel Institute, Washington, D. C.

Danza, M. A. and Murray, T. M. (1998). "Lateral Restraint Forces in Quarter-point and Third-point Plus Support Braced Z-purlin Supported Roof Systems," Research Report CE/VPI-ST-99/07, Department of Civil and Environmental Engineering, Virginia Polytechnic Institute and State University, Blacksburg, Virginia.

Elhouar, S., & Murray, T. M. (1985) "Prediction of Lateral Restraint Forces for Z-Purlin

Supported Roof Systems," Fears Structural Engineering Laboratory, Report No. FSEL/AISI 85-01. University of Oklahoma, Norman, Oklahoma.

Ghazanfari, A. and Murray, T. M. (1983). "Prediction of Lateral Restraint Forces of Single Span Z-purlins with Experimental Verification," Fears Structural Engineering Laboratory Report No. FSEL/MBMA 83-04, University of Oklahoma, Norman, Oklahoma.

Seshappa, V., & Murray, T.M. (1985) "Experimental Studies of Z-Purlin Supported Roof Systems Using Quarter Scale Models," Fears Structural Engineering Laboratory, Report No. FSEL/MBMA 85-02. University of Oklahoma, Norman, Oklahoma.

Specification for the Design of Cold-Formed Steel Structural Members (1996). American Iron and Steel Institute, Washington, D.C.

Zetlin, L. & Winter, G. (1955) "Unsymmetrical Bending of Beams with and without Lateral Bracing," Proceedings of the American Society of Civil Engineers, Vol. 81, pp. 774-1 to 774-20.

APPENDIX II. NOTATION

The following symbols are used in this paper:

a = spacing between purlin lines

b = purlin flange width

d = purlin depth

G' = roof panel shear stiffness (N/mm)

I_x = the moment of inertia with respect to the centroidal axis perpendicular to the web of the Z-section

I_{xy} = the product moment of inertia

L = span length

n_p = number of parallel, restrained purlin lines

P_L = restraint force

t = purlin thickness

T = total torque per purlin span

w = distributed gravity load along each purlin (force/length)

Δ = in-plane deflection of roof panel under point shear loading

θ = roof slope (from horizontal)

θ_0 = roof slope where restraint force is zero

θ_p = angle between purlin web and major principle axis of cross-section

APPENDIX III: PROPOSED Z-PURLIN RESTRAINT DESIGN PROCEDURE

$$P_L = P_0 C_1 \left(n_p^* \alpha + n_p \gamma \right)$$

where

$$P_0 = \left[\left(\frac{I_{xy}}{2I_x} + \frac{b}{3d} \right) \cos\theta - \sin\theta \right] W_p$$

$$W_p = wL$$

$$\alpha = 1 - C_2 \left(\frac{t}{d} \right) \left(n_p^* - 1 \right)$$

$$n_p^* = \min\{ n_p, n_{p(\max)} \}$$

$$n_{p(\max)} = 0.5 + \frac{d}{2C_2 t}$$

$$\gamma = C_3 \log\left(\frac{G'}{440 \text{ N/mm}} \right)$$

28

Table 5. Design Equation Coefficients

Configuration	C_1	C_2	C_3
Support Restraints:			
SS	0.50	5.9	0.35
MS, exterior	0.50	5.9	0.35
MS, interior	1.00	9.2	0.45
Third-point Restraints:			
SS	0.50	4.2	0.25
MS, exterior	0.50	4.2	0.25
MS, interior	0.45	4.2	0.35
Midspan Restraints:			
SS	0.85	5.6	0.35
MS, exterior	0.80	5.6	0.35
MS, interior	0.75	5.6	0.45
Quarter-point Restraints:			
SS, exterior	0.25	5.0	0.35
SS, interior	0.45	3.6	0.15
MS, exterior ¼ span	0.25	5.0	0.40
MS, interior ¼ span	0.22	5.0	0.40
MS, ½ span	0.45	3.6	0.25
Third-point Plus Support Restraints:			
SS, exterior	0.17	3.5	0.35
SS, interior	0.35	3.0	0.05
MS, exterior support	0.17	3.5	0.35
MS, interior support	0.30	5.0	0.45
MS, third-point	0.35	3.0	0.10

Notes:

1) Positive P_L is in tension, negative P_L is in compression.

2) Upper bound: $\left| P_L \right| \le \left| n_p P_0 C_1 \right|$

3) If $\left| P_L \right| \le 445\,\text{N}\,(100\,\text{lb})$, no lateral bracing is necessary.

4) Applicable range of panel stiffnesses:

$175\,\text{N/mm}\,(1000\,\text{lb/in.}) \le G' \le 17{,}500\,\text{N/mm}\,(100{,}000\,\text{lb/in.})$

5) C_1, C_2, and C_3 are regression coefficients.

6) Models used to develop procedure had $n_p \le 8$.

American Iron and Steel Institute

1140 Connecticut Avenue, NW
Suite 705
Washington, DC 20036

www.steel.org

The New Steel